

Experimental Analysis of Dissimilar Metals Welding

BOOPATHI K

BE- MECHANICAL

Shree Venkateshwara Hi-Tech
Engineering college, Gobi-
638455, Erode, Tamil Nadu.

boopathiboopathi1747@gmail.com

NITHYANANTHAN V

BE- MECHANICAL

Shree Venkateshwara Hi-Tech
Engineering college,
Gobi638455, Erode, Tamil Nadu.

Karthickkd509@gmail.com

PUVINTHARAJ P

BE- MECHANICAL

Shree Venkateshwara Hi-Tech
Engineering college,
Gobi638455, Erode, Tamil Nadu.

Karthickkd509@gmail.com

ABSTRACT

This study investigates the optimization of CO2 laser beam welding process parameters on dissimilar metal joint through CO2 laser beam welding of dissimilar metals namely low carbon steel AISI 1018 and austenitic stainless steel AISI 316L were investigated. Laser power, welding speed and shielding gas flow rate were considered as process parameter for this study. Effect of varying process parameters and interaction effect of process parameters on ultimate tensile strength were studied through analysis of experimental data. The second order quadratic model was used to predict optimum process parameters of laser beam welding. The optimum process parameter was observed at Laser power (599.99W), welding speed (100.15 mm/min) and shielding gas flow rate (1.7 bar). A conformation experiment was also conducted in order to validate the optimal process parameters values. The model found statistically fit for 95% confidence level. Keywords: Laser Beam Welding, Optimization, Dissimilar metals, Tensile strength

INTRODUCTION

The field of welding plays a crucial role in the fabrication of various structures across industries, ranging from aerospace to automotive and beyond. In welding, the joining of dissimilar metals presents unique challenges and opportunities due to differences in material properties, thermal expansion coefficients, and compatibility. The experimental analysis of dissimilar metals welding serves as a vital endeavor aimed at understanding, optimizing, and advancing the welding processes involved in joining metals with distinct compositions and characteristics.

This study focuses on investigating the intricacies of dissimilar metals welding through rigorous experimental analysis. By examining factors such as heat input, welding parameters, joint design, and material compatibility, researchers aim to elucidate the complex interactions occurring at the weld interface.

Through systematic experimentation and data analysis, this research seeks to uncover optimal welding techniques, mitigate potential defects, and enhance the mechanical properties of welded joints. Furthermore, the experimental analysis of dissimilar metals welding contributes to addressing industry demands for lightweight, high-strength materials and innovative fabrication techniques. By bridging the gap between theory and practice, this research endeavours to advance the state-of-the-art in welding technology, paving the way for the fabrication of novel structures and components with superior performance and durability. In this introduction, we will explore the significance of experimental analysis in understanding dissimilar metals welding processes, outline the objectives of the study, and highlight its potential implications for various industries and applications.

LITERATURE SURVEY

Over the years, significant research has been conducted in the field of dissimilar welding, yielding valuable insights into the challenges encountered in this domain. With dissimilar welding finding applications in nuclear, petrochemical, electronics, and various industrial sectors, this section presents a compilation of the contributions by researchers in this field. Chengwu et al. [1] investigated the weld interface microstructure and mechanical properties of copper-steel dissimilar welding. Their experimental findings revealed that a transition zone with numerous filler particles near the interface was observed for welded joints with a high dilution ratio of copper. Conversely, a low dilution ratio of copper resulted in the generation of the transition zone only near the upper side of the interface. Moreover, turbulent bursting behavior in the welding pool led to liquid metal penetration into copper at the lower side of the interface. Welded joints with lower dilution ratios of copper exhibited higher tensile strength [1]. They highlighted the potential failure of structures due to crack growth in both welds and the heat-affected zone (HAZ). Using a non-linear thermoplastic finite element model, they simulated a

circumferential weld in a thinwalled stainless steel pipe. Their findings indicated that choosing the appropriate hardening model, such as kinematic hardening, was crucial, especially in lowcycle simulations like few-pass welding processes. The study revealed that even under high thermal loads, the plasticity induced by thermal stresses might not sufficiently counteract the influence of weld residual stresses on CTOD, necessitating relaxation of residual stresses through unloading from primary tensile loads [2]. Mai and Spowage [3] conducted a characterization study of dissimilar joints, focusing on steel-Kovar, copper-steel, and aluminum-copper combinations. Colegrove et al. [4] investigated the impact of the welding process on residual stress and distortion. Their study aimed to elucidate the relationship between heat input, fusion area, measured distortion, and predicted residual stress from a simple numerical model, validated with experimental data. They highlighted that residual stress arises from the compressive yielding around the molten zone during material heating and subsequent contraction during cooling. This process results in a longitudinal tensile residual stress across the weld center line post-welding, which can decrease fatigue strength and toughness, particularly when combined with weld-related defects [4]. In conclusion, the body of research in dissimilar welding underscores the critical considerations of residual stress, microstructure development, and mechanical properties. These factors play pivotal roles in the integrity, performance, and reliability of welded structures across various industrial applications.

EXPERIMENTAL PROCEDURE

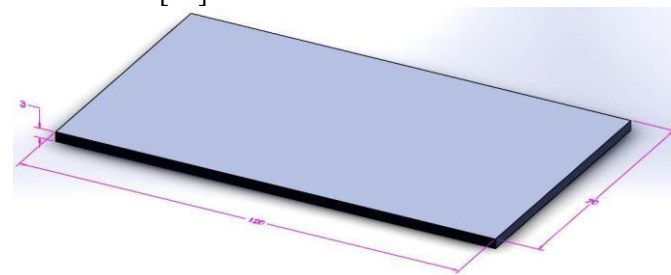
3.1 Laser welding

The CO₂ laser is commonly used type of solid-state laser in many fields at present because of its good thermal properties and easy repairing. The generation of short pulse duration in laser is one of the researcher areas. CO₂ is chosen for most materials processing applications because of the high pulse repetition rates available [7]. The power supply of pulsed CO₂ laser is designed to produce a maximum average power. CO₂ laser can be used for direct energy conduction welding of metals and alloys; the absorptive of metals increases as wavelength decreases. Since conduction welding is normally used with relatively small components, the beam is delivered to the work piece via a small number of optics. Simply beam defocusing to a projected diameter that corresponding to the size of weld to be made [7].

Base Materials

The rectangular specimens are equally prepared with a size of 100mm (length) x 75 mm (width) x 3mm (thickness) austenitic stainless steel AISI 316L to low carbon steel AISI 1018 specimens. The austenitic stainless steel 316L presence of nickel (11.9%), along with chromium (16.25%), enhances its corrosion [10,

for making the super heater and economizer. The cost of alloy steel is very high and hence in order to reduce the cost, the alloy steels may be mutual with low carbon steel [12].



Most commonly used austenitic stainless steel contain 18% chromium and 8% nickel.

3.1.3 Laser source

The CO₂ laser welding system was used and presented in Fig. 2. The laser beam having a maximum peak power 10 kW and standard pulse to pulse stability $\pm 3\%$. The laser fibre diameter 600 μm and standard fibre length 10 m. The laser beam was focused by using a copper mirror of focus length 200 mm.

3.1.4 Shielding Gas

The pure Argon gas at flow rate of 1.5 bar to 2.5 bar are supplied through a tube of 4 mm diameter in experimentation purpose with the nozzle angle 45° and standoff distance being 5 cm. **Process parameters and their actual values**

Factors	Notation	Unit	Factor Level		
			Low	Medium	High
Laser power	P	W	580	590	600
Welding Speed	S	m/min	100	150	200
Gas flow rate	G	bar	1.5	2	2.5

Tensile observations

The transverse tensile specimens are prepared as per ASTM E8M-04 guidelines and the specimens after wire cut Electro Discharge Machining. Tensile tests are carried out in Universal Testing Machine.

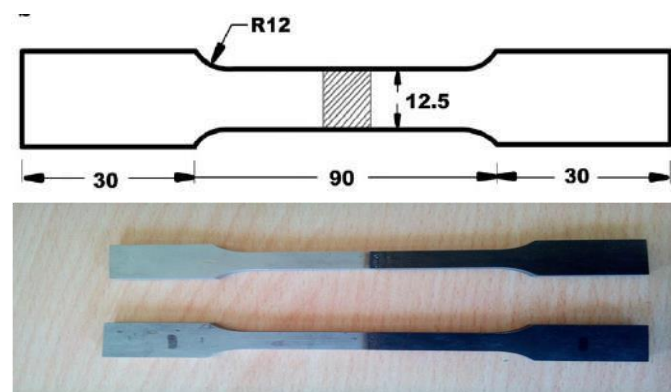
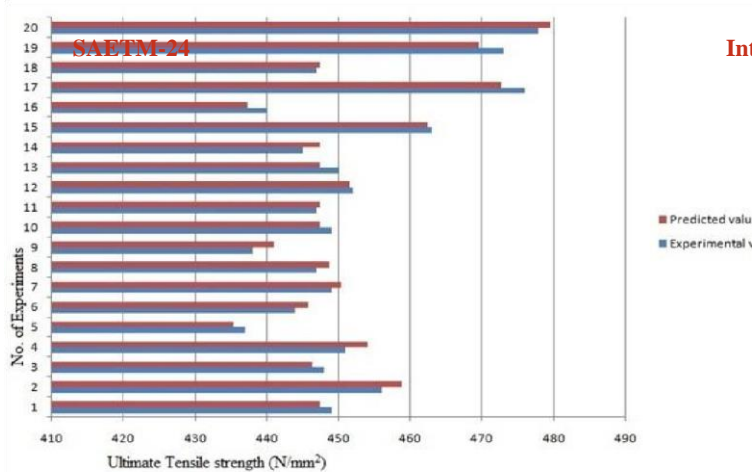


Figure:5 Tensile Test Specimen

A total of twenty experiments were conducted at different levels of parameters to obtain a laser beam welded joints of specimens. The values of weld



strength obtained from experiments and those predicted from response surface model are tabulated in table 4.

3.4 Response Surface Model for Weld Strength

The polynomial equation for the three factors considered in the present case is.

$$y_i = \beta_0 + \sum_{j=1}^q \beta_j x_j + \sum_{j=1}^q \beta_{jj} x_j^2 + \sum_{i < j}^3 \beta_{ij} x_i x_j \dots \dots \dots 1$$

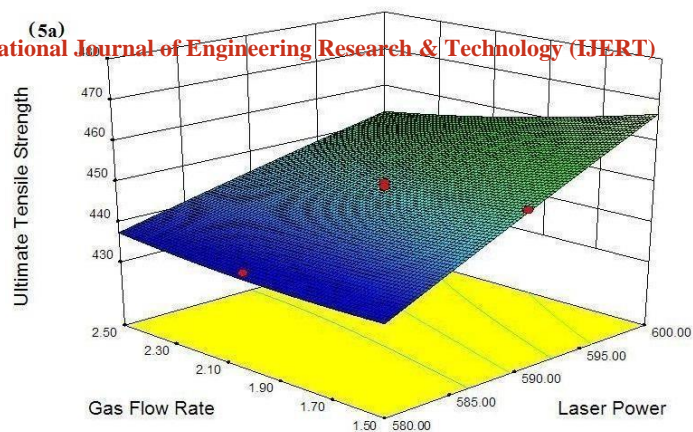


Figure: 9 Response surface due to interaction of laser power and travel speed on ultimate tensile strength.

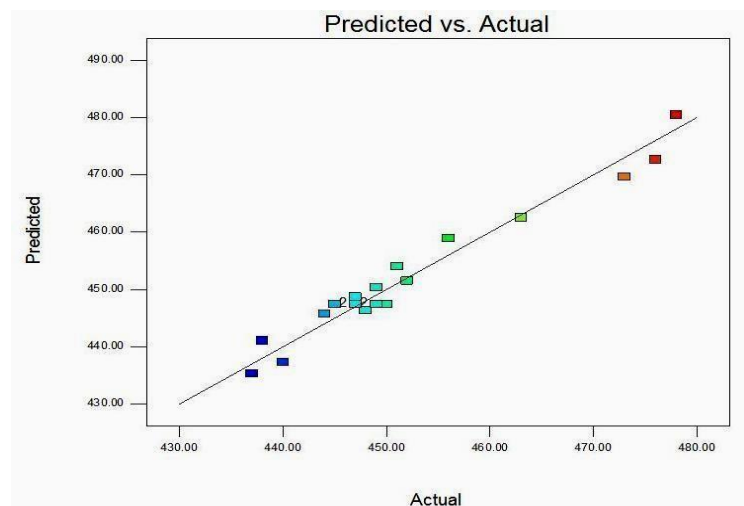
The laser beam welding input variables are laser power (P), Travel speed (S), Shielding gas flow rate (G) and PS, PG, SG, P², S², G² are interaction parameters.

$$\begin{aligned} \text{Ultimate Tensile Strength (UT)} = & 447.43 + 11.80 \times P - 6.90 \times S - 2.90 \times G - 0.32 \times P^2 + \\ & 8.18 \times S^2 + 1.18 \times G^2 - 1.38 \times PS - 3.88 PG \times - \\ & 2.88 \times SG \dots \dots \dots 2 \end{aligned}$$

RESULTS AND DISCUSSION

ANOVA

The ANOVA analysis indicates that the most significant parameters of the laser beam welding of 6mm thickness dissimilar welding factor when considering the ultimate tensile strength. Mathematical predictive model of response surface methodology approach has been developed to accurately predict the desire responses.



Response Surface Graphs

The response surfaces clearly indicate the optimal response point and the different collared surfaces show that the value of ultimate tensile strength obtained for the corresponding values of input parameters. Response surface graphs for the response of ultimate tensile strength obtained from the regression model.

Figure: 8 Response surface due to interaction of laser power Figure 8 show the response surface graphs for the

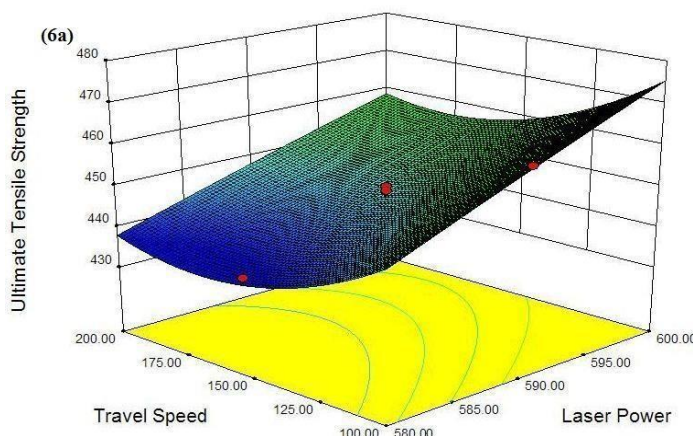
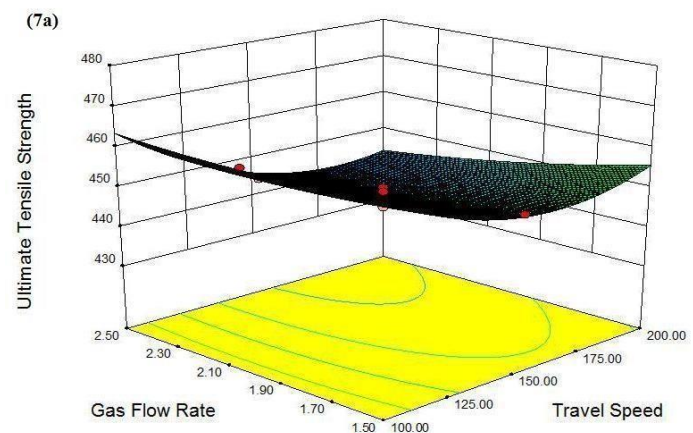


Figure: 10 Response surface due to interaction of travel speed and gas flow rate on ultimate tensile strength.



ultimate and gas flow rate on ultimate tensile strength. tensile strength between laser power (P) and gas flow rate

(G) obtained from the regression model. The ultimate tensile strength is increasing with increasing of laser power (P) and decreasing of shielding gas flow rate (G). The penetration depth increases with increasing laser power, Low heat input laser welds resulted in significant variation in the ferrite / austenite balance of fusion zone 9 show response surface obtained from the regression model, approximately welding speed ($S = 100.15$ mm/min) and laser power ($P = 599.99$ W) gives the optimum ultimate tensile strength ($UT = 478$ N/mm²) apex of the response surface [5]. The least amount fusion zone produced by laser beam is depended on heat input as a function of laser power and welding speed. The nature of ferrite to austenite transformation in fusion zone is strongly influenced by cooling rate, which is depended on heat input as a function of laser power and welding speed. The ultimate tensile strength improved with either increasing laser power or decreasing welding speed that means with increasing heat input. The response surface graphs for ultimate tensile strength between welding speed and shielding gas flow rate, it can be seen from this figure 10 that ultimate tensile strength increases with decreasing of travel speed(S) [9] and decreasing of shielding gas flow rate (G). The interaction between LBW process parameters on travel speed ($S = 100$ mm/min) and shielding gas flow rate ($G = 1.1$ bar) gives maximum ultimate tensile strength ($UT = 463$ N/mm²). Shielding gases enhances and promotes a dendritic structure in the weld metal, and it is also endowed with a higher amount of secondary interdimeric austenite phase [13]. A laser welding with an argon gas shielding is that generated plasma on the plate heats itself. Any values of shielding gas flow rate and minimum amount of travel speed produce high ultimate tensile strength obtained from the response surface graph.

Microstructure and EDAX In order to observe the microstructure under SEM specimens were cut from the weld by the wire cut EDM process and sample were prepared. A scanning electron microscope (SEM) is a type of electron microscope that produces images of a sample by scanning it with a focused beam of electrons. The electrons interact with atoms in the sample, producing various signals that can be detected and that contain information about the sample's surface topography and composition.

Energy-dispersive X-ray spectroscopy (EDS, EDX, or XEDS) is an analytical technique used for the elemental analysis or chemical characterization of a sample. Its characterization capabilities are due in large part to the fundamental principle that each element has a unique atomic structure allowing unique set of peaks on its Xray spectrum. To stimulate the emission of characteristic X-rays from a specimen, a high-energy beam of charged

relative to the base metal as a consequence of high cooling rate. When the laser power below ($P = 599.9$ W) ultimate tensile strength was gradually decreased on other hand when the laser power increasing gradually within limit the ultimate tensile strength increases it is indicated from the response surface graph [8,6]. Figure particles such as electrons or protons or a beam of X-rays, is focused into the sample. An atom within the sample contains ground state electrons in discrete energy levels or electron shells bound to the nucleus. An electron from an outer, higher-energy shell then fills the hole, and the difference in energy between the higher-energy shell and the lower energy shell may be released in the form of an X-ray. The number and energy of the X-rays emitted from a specimen can be measured by an energy-dispersive spectrometer. As the energy of the X-rays is characteristic of the difference in energy between the two shells, and of the atomic structure of the element from which they were emitted, this allows the elemental composition of the specimen to be measured.

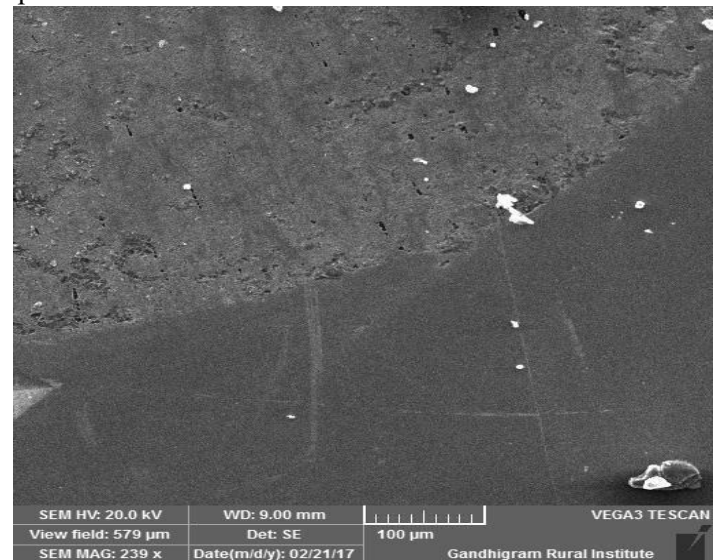


Figure 12 Micro structure of welded zone

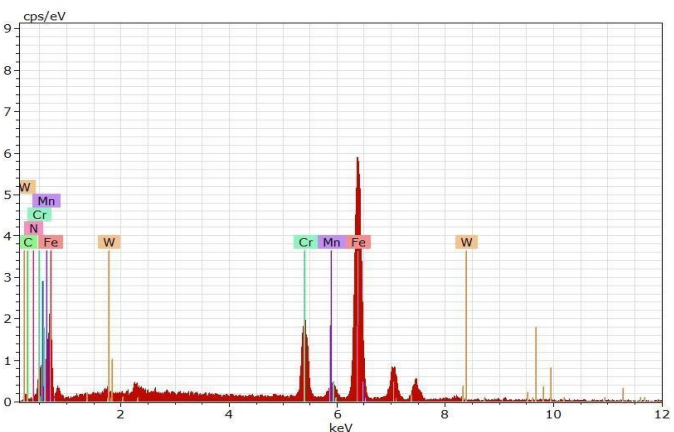


Figure 13 Presentation of Energy Dispersive X-ray Spectroscopy line analyses.

APPLICATION

Application of Austenitic Stainless Steel AISI 316L To Low Carbon Steel AISI 1018

Marine Engineering: Components such as ship hulls, offshore platforms, and marine equipment benefit from the corrosion resistance of AISI 316L stainless steel when welded to low carbon steel. This combination ensures durability and longevity in harsh marine environments.

Chemical Processing: Tanks, pipelines, and equipment used in chemical processing plants require materials that can withstand corrosive substances. Welding AISI 316L to AISI 1018 allows for the construction of durable structures capable of withstanding corrosive chemicals.

Food Processing: Equipment in food processing facilities must meet stringent hygiene standards while resisting corrosion from food products and cleaning chemicals. Welded joints between AISI 316L and AISI 1018 provide the necessary corrosion resistance and mechanical strength for such applications.

Automotive Industry: Various automotive components, such as exhaust systems and chassis parts, benefit from the combination of strength and corrosion resistance achieved by welding AISI 316L to AISI 1018. This combination ensures durability and reliability in automotive applications. **Structural Engineering:** Welding dissimilar materials like AISI 316L and AISI 1018 allows for the construction of structures with optimized performance characteristics. This can include bridges, building frameworks, and other structural components where a balance between strength, corrosion resistance, and cost-effectiveness is essential. **Oil And Gas Industry:** Pipelines, storage tanks, and equipment used in the oil and gas industry are subjected to harsh environmental conditions and corrosive substances. Welding AISI 316L to AISI 1018 provides a solution that meets the industry's requirements for corrosion resistance and mechanical strength.

Heat Exchangers: Heat exchangers used in various industries, including HVAC systems, chemical processing, and power generation, often require materials that can withstand high temperatures and corrosive environments. Welding AISI 316L to AISI 1018 allows for the construction of heat exchangers with enhanced corrosion resistance and thermal conductivity.

Overall, the welding of austenitic stainless steel AISI 316L to low carbon steel AISI 1018 specimens find applications across a wide range of industries where a combination of corrosion resistance, mechanical strength, and cost-effectiveness is necessary.

CONCLUSION

In this study investigates the optimization of laser beam welding process parameters through Response Surface Methodology (RSM) based on central composite face centred design. Laser beam welding process parameters like laser power, welding speed and shielding gas flow rate on the maximum ultimate tensile strength of dissimilar metal joints were determined in this parametric study. The maximum ultimate tensile strength (478.02 N/mm²)

obtained by the conditions like laser power (599.99 W), shielding gas flow rate (1.70 bar) and low travel speed (100.15 mm/min). A conformation experiment was also conducted in order to validate the optimal process parameters values. The developed relationship can be effectively used to predict the ultimate tensile strength of laser beam welded joints at 95% confidence level.

REFERENCES:

- [1]. Chengwu et al, July–August 2009, Interface microstructure and mechanical properties of laser welding copper–steel dissimilar joint, Elsevier, Pages 807-814. [2]. Delphin, Sattari-Far and Brickstad, June 2009, studied the effect of thermal and weld residual stresses on CTOD, Kostas Xanthopoulos, 54-57.
- [3]. Mai and Spowage, June 2004, characterisation of dissimilar joints of steel-Kovar, copper-steel and aluminium copper, Beowulf, 224-233.
- [4]. Colegrove et al, November 2009, welding process impact on residual stress and distortion welding process impact on residual stress and distortion, Bhagavad Gita, 717-725.
- [5]. Delphin et al, January 2003, Combined hardening and softening constitutive model of plasticity: Precursor to shear slip line failure, 88- 100, Computational Mechanics 31(1). [6]. Paventhan R, Lakshminarayanan P R, Balasubramanian V., (2011) Prediction and optimization of friction welding parameters for joining aluminium alloy and stainless steel. Transactions of Nonferrous Metals Society of China, 21: 1480–1485.
- [7]. F. Curcio, G. Daurelio, F. Memola Capece Minutolo (2006) “On the welding of different materials by diode laser”. Journal of Material Processing Technology, 175: 8389.
- [8]. Huang Q, Hagstroem J, Skoog H, Kullberg G (1991) Effect of CO₂ laser parameter variations on sheet metal welding. Int J Join Mater 3 (3): 79-88.
- [9]. Mai TA, Spowage AC (2004). Characterisation of dissimilar joints in laser welding of steel-kovar, copper-steel and copper-aluminium. Material science and engineering, A 374: 224-233.
- [10]. G Vairamani, T. Senthil kumar, S. Malarvizhi, V. Balasubramanian (2013) “Application of response surface methodology to maximize tensile strength and minimize interface hardness of friction welded dissimilar joints of austenitic stainless steel and copper alloy”. Trans. Nonferrous Met. Soc. China 23 2250-2259. [11]. Wang HY, Li ZJ (2006) “Investigation of laser beam welding process of Az61 magnesium-based alloy”. Acta Metall Sin 19 (4): 287-294.
- [12]. T. A. Mai, A. C. Spowage (2004) “characterisation of dissimilar joints in laser welding of Steel- Kovar/ Copper-Steel and Copper-Aluminium”. Journal of Material Science and Engineering, A374 224-233.
- [13]. Paulraj Sathiya, M. Y. Abdul Jaleel (2011) “Influence of shielding gas mixtures on bead profile and microstructural characteristics of super austenitic stainless steel weldments by laser welding”. Int J Adv Manuf Technol 54:5-22.

[14] Arunraja KM, Selvakumar S, Praveen P (2019) Optimisation of welding fixture layout for sheet metal components using DOE. *Int J Prod Qual Manag* 28(4):522–558

[15] J . Yasin, S. Selvakumar, P.M. Kumar, R. Sundaresan, and K.M. Arunraja, Experimental Study of TiN, TiAlN and TiSiN Coated High Speed Steel Tool, *Mater. Today Proc.*, 2022, 64, p 1707–1710.
<https://doi.org/10.1016/j.matpr.2022.05.468>

[16] Mathivanan, S., K. M. Arunraja, and M. Viswanath. "Experimental Investigation on Aluminum Metal Matrix Composite." *International Journal of Engineering Research & Technology*, ISSN (2018): 2278- 0181.